DESIGN CONSIDERATIONS FOR DC SQUIDS FABRICATED IN DEEP SUB-MICRON TECHNOLOGY

M.B. Ketchen
IBM Research Division, T.J. Watson Research Center
Yorktown Heights, New York 10598

Abstract

Design rules for scaling dc SQUID junctions to optimize SQUID performance have been well known for over a decade, and verified down to the sub-micron regime. Practical SQUIDs having well coupled input coils of useable inductance have generally been fabricated at the 2 - 5 μm level of lithography. Other technologies, silicon in particular, are now routinely practiced at the 0.5 μm level of lithography with impressive demonstrations at the 0.1 - 0.25 μm level not uncommon. In this paper the implications of applying such fabrication capability to advance dc SQUID technology are explored. In particular the issues of scaling practical dc SQUIDs down to the 0.1 - 0.25 μm regime are examined, using as a prototype design the basic washer SQUID with a spiral input coil[1]. A technical path is mapped out that leads to a practical SQUID less than 0.05 mm^2 in area with a tightly coupled 2 μH input coil, user friendly voltage - flux characteristics, minimal flux creep related hysteresis, and coupled energy sensitivity approaching the quantum limit at 4.2 K.

Introduction

There are two major sets of issues involved in scaling practical dc SQUID designs into the deep sub-μm regime. The first involves the scaling of Josephson elements and associated resistors and contacts. The second concerns the scaling of input coil dimensions and the configuration of the SQUID inductance.

The white noise and scaling properties of Josephson elements, tunnel junctions in particular, have been the subject of considerable calculation[2] and experiment, with a good understanding now in hand. Nevertheless, it has been only very recently that the basic theory has been shown to hold for SQUIDs fabricated in $Nb-AlOx-Nb$ trilayer technology[3,4] that simultaneously have very low 1/f noise[5]. Since from a materials and processing standpoint such technology is a leading candidate for scaling, we will briefly summarize the scaling projections for the white noise performance in this technology. We will also discuss some of the more practical issues of scaling resistors and contacts, minimizing parasitic capacitance, and incorporation of a damping resistor to retain smooth, well-behaved voltage-flux characteristics.

While much work has been devoted to scaling of tunnel junctions to small dimensions little effort has been directed to scaling SQUID input coils to sub-μm linewidths. Practical planar SQUIDs[1,6] typically have input coils with linewidths of 2-5μm, most with input coil inductances well below the industry standard of $2\mu H$. If one has the technology to fabricate deep sub-μm tunnel junctions, one may (or may not) also have the technology to fabricate very fine line input coils. Such coils, assuming they retain good coupling characteristics, will provide some important advantages. For fixed SQUID inductance L and input coil inductance L_i the size of the SQUID reduces rapidly with the linewidth of the input coil. This will lead to a higher density of SQUIDs on the wafer and improved economy of scale. It has been the experience in the semiconductor industry that, assuming it can be fabricated at all, a scaled design most often has higher yield than the original. It will also be possible to accommodate a full 2μH input coil on a physically small washer where parasitics are not a major concern. In addition, as the aspect ratio of the washer decreases, magnetic flux penetration related problems such as hysteresis and certain temperature dependencies will moderate. This will make the SQUIDs much more attractive for operation in the earth's field. We will revisit the issues of planar coupling for the washer SQUID design and discuss the details of how the coupling continues to work into the deep sub-μm regime.

Manuscript received September 24, 1990.

SQUID Noise and Junction Scaling Considerations

A figure of merit commonly used to compare SQUIDs is the coupled energy sensitivity[7,8]

$$\varepsilon_c = \frac{\varepsilon}{k^2} = \frac{\phi_n^2}{2k^2 L} \,, \tag{1}$$

where ε is the intrinsic energy sensitivity, ϕ_n is the flux noise and $k^2 = M_i^2/L_i L$, M_i being the mutual inductance between L and L_i. The intrinsic energy sensitivity in the white noise region is predicted to be[2,9]

$$\varepsilon = \gamma_1 h\left(\frac{k_B T}{e I_0 R}\right) + \gamma_2 h \,, \tag{2}$$

where the prefactor $\gamma_1 \approx 3-5$, and γ_2, the prefactor of the quantum contribution, is thought to be $\sim$0.2. In the case of tunnel junctions R is the value of the shunt resistor that must be placed across each junction to ensure non-hysteretic behavior. The value of ε in the low frequency (typically 1/f) noise regime, while of great importance for many applications, is not easy to predict and tends to depend on the details of the technology in ways that are not always well understood. For today's laboratory produced SQUIDs at the 2μm technology level, values of ε_c in the white noise region at 4.2K in the range of 10-100h are common. Today's best commercially available SQUIDs have $\varepsilon_c \approx 1500h$.

Design rules for scaling SQUID junctions to obtain very low values of ε in the white noise region were developed[2] in the 1970's and verified down to the vicinity of the quantum limit on experimental devices as early as 1982[10]. Two key design equations are

$$\beta_L = \frac{2LI_0}{\phi_0} = 1 \tag{3}$$

and

$$\beta_c = 2\pi I_0 R^2 C/\phi_0 \lesssim 1 \,, \tag{4}$$

where C is the junction capacitance, including parasitics. Equation (3) provides for an optimum critical current modulation depth of $\sim$50% while Eq. (4) ensures non-hysteretic device characteristics[11,12]. Equations (3) and (4) together with Eqs. (1) and (2) provide the basic framework for scaling.

The best way to predict white noise performance for a given technology is to scale from the known performance of an existing SQUID built in that technology. In the case of $Nb-AlOx-Nb$ we have known performance[5] of $\varepsilon(4.2K) = 6h$ in the white noise region, with a white to $1/f$ crossover frequency below 10Hz, for a device with I_0R = 225μV and j_c of 600 A/cm^2. This SQUID had $L = 50pH$, $I_0 = 16\mu A$, $R = 14\Omega$, and junction area $\mathscr{A} = 3\mu m^2$; with $\beta_c \approx 1$, $C \approx 0.12pF$. For our practical design we will hold L constant at 100 pH which implies $I_0 \approx 10\mu A$. Using our known case and the scaling equations we first calculate a reference case for 1 μm^2 junctions from which it will be a straightforward matter to scale further. For our reference case we then have $\mathscr{A} = 1\mu m^2$, $j_c = 10^3 A/cm^2$, $R = 30\Omega$, and $I_0R = 300\mu V$, and ε(4.2K) = 5h. The set of equations that then prescribes our scaled design as a function of the current density j_c is:

$$L = 100pH \tag{5}$$

$$I_0 = 10\mu A \tag{6}$$

$$\mathscr{A} = 1\mu m^2\left(\frac{10^3 A/cm^2}{j_c}\right) \tag{7}$$

$$R = 30\Omega\left(\frac{j_c}{10^3 A/cm^2}\right)^{1/2} \tag{8}$$

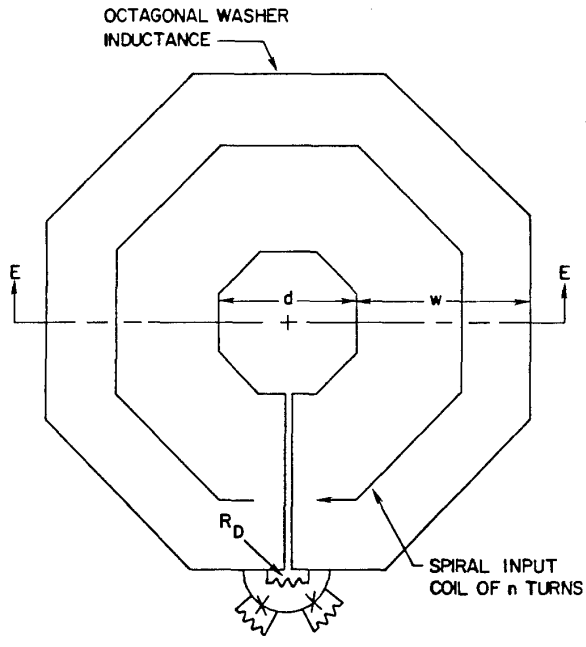

Fig. 1 Octagonal washer dc SQUID design.

$$I_0R = 300\mu V\left(\frac{j_c}{10^3 A/cm^2}\right)^{1/2} \tag{9}$$

$$\varepsilon(4.2K) = 5h\left(\frac{10^3 A/cm^2}{j_c}\right)^{1/2}, \tag{10}$$

where we have assumed that the specific capacitance of the junction is independent of j_c and that parasitic capacitance in parallel with the junctions remains negligible.

To insure smooth, well behaved voltage - flux characteristics, especially with a tightly coupled input coil, it is advisable to place a damping resistor R_D across the SQUID inductance as indicated in Fig 1. The value of R_D should be 2-3 times that of R so that the thermal noise associated with R_D will not contribute significantly to ϕ_n[13]. We thus add one final equation to describe our design:

$$R_D = 75\Omega\left(\frac{j_c}{10^3 A/cm^2}\right)^{1/2}. \tag{11}$$

The implications of this set of scaling equations is fairly self evident. At $j_c = 10^5 A/cm^2$ we will require 0.01 μm^2 junctions, $R = 300\Omega$, and $R_D = 750\Omega$. I_0R will increase to the gap voltage of 3mV, and $\varepsilon(4.2K)$ will be about 0.5h. Even if we back off a factor of two in resistance values to make $\beta_c \ll 1$ and add considerable process latitude, $\varepsilon(4.2K)$ will be of order h. We have no real basis for predicting how the 1/f noise will behave as we scale. Nevertheless the excellent 1/f noise preformance of $Nb - AlOx - Nb$ SQUIDs at $> 1\mu m$ gives us reason to be optimistic.

Current densities of 10^5 A/cm^2 for $Nb - AlOx - Nb$ junctions are obviously very high, but not out of the question. Junctions at $j_c = 2.4 \times 10^4$ A/cm^2 and $\mathscr{A} < 0.01\mu m^2$ were recently reported[14]. Even if one elects to go with 10^4 A/cm^2 the projected SQUID performance is excellent with ε (4.2K) $\approx$ 1.5h.

For the scaling projections to hold, it is essential that C be dominated by the actual junction capacitance C_j and not by parasitic capacitance C_p. The value of C_p will depend critically upon the details of the junction structure. A simple overlap configuration, for example, can have extremely low C_p; however, the junction area can then become a critical function of the lithographic overlay[14]. In the case of a trilayer junction, the situation is typically as shown

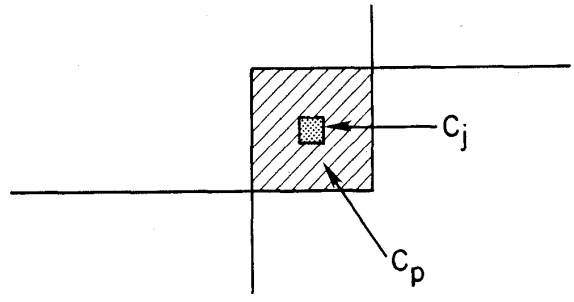

Fig. 2 Trilayer junction with self-aligned oxide.

in Fig. 2[3,4,15,16]. There is a patterned base electrode, a junction incorporated in a counterelectrode pedestal, an oxide self-aligned at the pedestal, and a contact level that connects to the counterelectrode. One way to configure a SQUID is to form the washer out of the contact level while patterning the input coil in the base electrode. Shunt resistors can, for example, be wired up with the contact level, connection to the junction base electrode being made through a large "contact" junction.

In the arrangement shown in Fig. 2 there is obviously a parasitic capacitance in parallel with C_j that depends on the thickness and dielectric constant of the self-aligned oxide and upon the overlap area of the base electrode and contact level. 0.1μm thick sputtered quartz will give $\sim 0.3fF/\mu m^2$ while the same thickness of Nb_2O_5 will give $\sim 2fF/\mu m^2$. For a 0.01 μm^2 junction with a sputtered quartz dielectric we can tolerate a worse case overlap of only about 0.1-0.2μm^2, which puts considerable demand on our processing control. The situation becomes even more demanding for higher dielectic constant insulators.

Resistors need to be carefully examined as well. If the resistors are wired up with the contact level, then they can be groundplaned with the base electrode. In the case of the shunt resistors, however, this would add substantial parasitic capacitance in parallel with C_j. One possible approach is to use ungroundplaned shunt resistors, 2μm in width, with a maximum length of 20μm. This gives a parasitic inductance well below L and leads to a reasonable maximum sheet rho requirement of about 30$\Omega/\square$. The maximum power density for the shunt resistor would be about 0.1W/cm^2 which is still an order of magnitude below resistor power densities commonly used for 4.2K Josephson logic circuits. More spread out resistor arrangements may be required for operation at temperatures significantly below 4.2K[17] The damping resistor R_D can be groundplaned by the base electrode to significantly lower parasitic inductance. The associated parasitic capacitance which is in parallel with L only adds incrementally to the already large capacitance associated with the turns of the input coil.

Square contacts between the contact level and the base electrode with current carrying capacity of up to j_c times the square of the Josephson penetration length are available at no additional processing cost. Such contacts easily meet shunt resistor requirements and actually become very compact at high current densities (ie. $\sim 1\mu m^2$ for 1 mA at 10^5A/cm^2). If higher currents are required, such as for contacts in input coil structures, it may be necessary to add another level of lithography for RIE of contact holes through the self aligned oxide down to the base electrode.

Inductance and Coupling Considerations

The layout of the washer and input coil for our SQUID are as depicted in Fig 1. The inductance of the washer SQUID can be written as

$$L = L_h + L_t + L_j, \tag{12}$$

where L_h is the inductance of the hole, L_t is the inductance of the slit, and L_j is the parasitic inductance associated with the junction region (typically a few pH). For a process with only 4-5 levels of lithography it is not possible to fully groundplane the slit, and L_t will not be negligible. One way of handling L_t is to treat the slit

as a two dimensional structure with a constant inductance per unit length $\mathscr{L}_t$. Under this assumption we have numerically calculated $\mathscr{L}_t$ as a function of various dimensions[18] and, as expected, find it to be an extremely weak function of the geometry. For slit dimensions of order 1μm, $\mathscr{L}_t \approx 0.4pH/\mu m$. There will actually be some partial groundplaning of the slit by the turns of the nearby spiral input coil. For practical situations we estimate $\mathscr{L}_t$ will be on the order of 0.3pH/μm, with little leverage in pushing hard to make the slit dimensions real small. For an 80μm long slit, L_t will then be about 24pH.

L_t is not a parasitic inductance in the sense of L_j since it partially couples to the turns of the input coil. In the presence of non-zero L_t, it can be shown that the expressions for M_i, L_i and k^2 are

$$M_i = n(L_h + L_t/2) \tag{13}$$

$$L_i = n^2(L_h + L_t/3) + L_s \tag{14}$$

$$k^2 = \frac{n^2(L_h + L_t/2)^2}{L\,[n^2(L_h L + L_t/3) + L_s]} =$$

$$\left[1 + \left\{\frac{L_h^2 + L_t L_h/4}{(L_h + L_t/2)^2}\right\}\frac{L_t}{3L_h} + \left\{\frac{L_h^2 + L_t L_h/3}{(L_h + L_t/2)^2}\right\}\frac{L_j}{L_h} + \left\{\frac{LL_h}{(L_h + L_t/2)^2}\right\}\frac{L_s}{n^2 L_h}\right]^{-1}, \tag{15}$$

where L_s is the stripline inductance of the coil with respect to the washer and the quantities within { }'s become unity in the limit of small L_t. There is an underlying assumption that the current in the input coil is nealy perfectly imaged in the washer and that at the slit the image current associated with each turn of the input coil completes its path by flowing around the inside edge of the washer's hole [1,9]. If $L_j = L_s = 0$ and we shrink the washer hole size to zero, we are left with a "slit SQUID" having $k^2 = 0.75$. For $L_t/L_h \approx 0.3$ we will suffer a loss in k^2 of about 8%.

The quantity L_s/n^2L_h in Eq. (15) is one we must examine carefully. Figure 3 shows the cross section EE taken through the washer SQUID in Fig. 1, with the vertical dimensions exaggerated and $n = 4$ for clarity. The linewidth and spacing for the coil are both a and the insulator thickness is s. The penetration depths of the coil

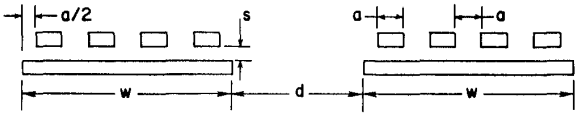

Fig. 3 Cross-section EE through the octagonal washer SQUID in Fig. 1. Vertical dimensions are exaggerated and the number of input coil turns has been reduced for clarity.

and washer are λ_1 and λ_2 respectively. The inductance of the octagonal washer of hole size d is approximately $1.05\mu_0 d$ provided the width of the washer w is greater than d[1,19]. In the limit of $s + \lambda_1 + \lambda_2 \ll a$ the stripline inductance per unit length $\mathscr{L}_s$ of the coil with respect to the washer is given by

$$\mathscr{L}_s = \mu_0\left(\frac{s + \lambda_1 + \lambda_2}{a}\right) \tag{16}$$

as can be shown with a simple application of Ampere's law. The average length of a spiral turn is $1.05\pi(d + w)$ so the total length of the spiral coil is $1.05\pi n(d + w)$. We can then express L_s/n^2L_h as

$$L_s/n^2L_h = \pi\left(\frac{d+w}{d}\right)\left[\frac{2a}{w}\left(\frac{s + \lambda_1 + \lambda_2}{a}\right)\right]$$

$$= 2\pi\left(\frac{d+w}{d}\right)\left(\frac{s + \lambda_1 + \lambda_2}{w}\right) \tag{17}$$

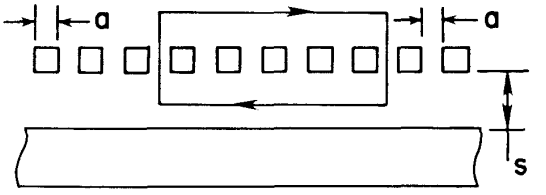

Fig. 4 Path of integration for applying Ampere's Law to calculate $\mathscr{L}_s$ in the limit $s + \lambda_1 + \lambda_2 \gg a \gg \lambda_1$. The situation is analogous to that of a long single layer solenoid of fine wire.

where we have used the fact that $n = w/2a$. As an example, for $d = 60\mu m$, $w = 80\mu m$, $s = 0.15\mu m$, and $\lambda_1 = \lambda_2 = 0.086\mu m$, $L_h \approx 80pH$ and $L_s/n^2L_h \approx 0.06$.

As a is made smaller fringing fields become important and Eq. (16) overestimates $\mathscr{L}_s$. On the other hand these fringing fields also start to couple turns directly to each other through leakage flux. The relevant $\mathscr{L}_s$ then becomes the strip line inductance per unit length plus the sum of all the leakage-flux-coupling-mutuals. This problem gets very complex rapidly, however, there is another limit in which it again becomes simple to analyze. That is the limit depicted in Fig. 4 where $s + \lambda_1 + \lambda_2 \gg a \gg \lambda_1$. The situation is then somewhat analogous to that of a solenoid wound of fine wire. We can again apply Ampere's law as indicated in Fig 4 to obtain

$$\mathscr{L}_s = \frac{\mu_0}{2}\left(\frac{s + \lambda_1 + \lambda_2}{a}\right), \tag{18}$$

where $\mathscr{L}_s$ now includes all the mutuals as well as the stripline inductance $\mathscr{L}_w$ of the line. The coupling has actually improved as we have reduced a ! To illustrate this effect in more detail we have calculated $\frac{a}{w}\mathscr{L}_w$ and plotted it in units of $\mu_0\left(\frac{s + \lambda_1 + \lambda_2}{2w}\right)$ as a function of a. For this calculation we have set $\lambda_1 = 0$, $\lambda_2 = 0.086\mu m$, and $s = 0.236\mu m$. The thickness of the coil is kept constant at 0.15μm until a reaches 0.15μm. Below 0.15μm the width and the thickness of the line are both set equal to a. The results of this calculation are shown in the $\frac{a}{w}\mathscr{L}_w(\lambda_1 = 0)$ curve of

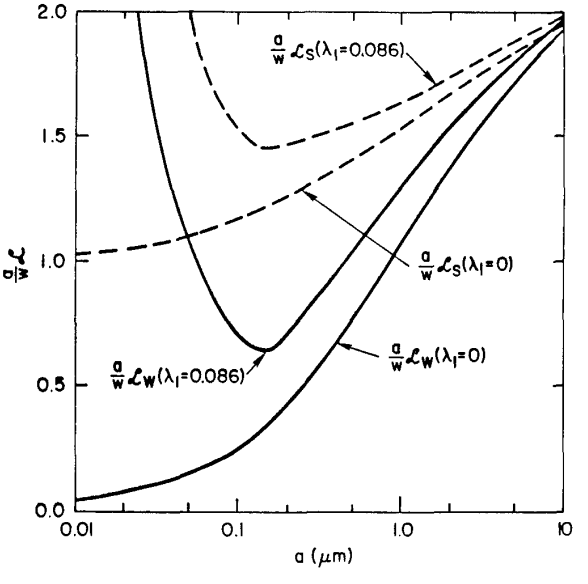

Fig. 5 $\frac{a}{w}\mathscr{L}$ in units of $\mu_0\left(\frac{s + \lambda_1 + \lambda_2}{2w}\right)$ as a function of a.

Fig. 5. For a large, $\frac{a}{w}\mathscr{L}_w(\lambda_1=0)\approx 2$ as expected. For $a \ll s+\lambda_1+\lambda_2$, $\frac{a}{w}\mathscr{L}_w(\lambda_1=0)\ll 1$. Since in this limit $\frac{a}{w}\mathscr{L}_s(\lambda_1=w)=1$, it is clear that $\mathscr{L}_s(\lambda_1=0)$ is dominated by the mutuals and not $\mathscr{L}_w$. $\frac{a}{w}\mathscr{L}_s(\lambda_1=0)$ has not been calculated, but the dashed line so labelled in Fig. 5 is an estimation of what this curve must look like.

In reality with $\lambda_1 \approx 0.086\mu m$, characteristic of Nb, it is difficult to get into the regime where $s+\lambda_1+\lambda_2 \gg a \gg \lambda_1$. As a is reduced to $\sim \lambda_1$ kinetic inductance begins to play a very significant role. To illustrate this we have calculated and plotted in Fig. 5 $\frac{a}{w}\mathscr{L}_w(\lambda_1=0.086\mu m)$ under the same set of assumptions as for the previous case, except that now $\lambda_1=0.086\mu m$ and $s=0.15\mu m$. The striking difference is the dramatic upturn and fast rise of $\frac{a}{w}\mathscr{L}_w(\lambda_1=0.086\mu m)$ as a is decreased below $0.15\mu m$. This quantity passes through 2 when $a \approx 0.05\mu m$. The mutuals will not be significantly different than in the $\lambda_1=0$ case, but $\mathscr{L}_w$ will now be the dominant contributor to $\mathscr{L}_s$ for very small values of a. As in the previous case $\frac{a}{w}\mathscr{L}_s$ has not been calculated, but the dashed curve for $\lambda_1=0.086$ in Fig. 5 is an estimation of what this curve must look like. $\frac{a}{w}\mathscr{L}_s$ is again nearly 2 for large a, but rather than smoothly reducing to 1 for small a as in the $\lambda_1=0$ case, it now turns around in the vicinity of $0.15\mu m$ and steeply rises though 2 in the vicinity of $a = 0.05\mu m$. The most interesting and important result from this exercise is that Eq. (17) remains as a valid upper bound on L_s/n^2L_h over the entire range of a from w down to $0.05\mu m$! Using Eq. (17) will give modest underestimates of k^2 for intermediate values of a. It also follows that since we have built washer SQUIDs with $a=2.5\mu m$ and n from 10 to 50 or more that work as predicted, the same SQUIDs with $a=0.25\mu m$ should couple just as well or better with L_i greater by a factor of 100.

As a practical example we consider an octagonal washer SQUID with $d=60\mu m$ and $w=80\mu m$. This SQUID will have $L_h \approx 80pH$, $L_i \approx 24pH$, and $L_j \approx 3pH$. The input coil with $0.25\mu m$ lines and spaces will have n=160 turns. Assuming $\lambda_1=\lambda_2=0.086\mu m$ and $s=0.15\mu m$ we use Eq. (17) to calculate $L_s/n^2L_h=0.06$. We also have $L_s/3L_h \approx 0.10$ and $L_j/L_h \approx 0.04$. Using Eqs. (12-15), we then calculate $L=107pH$, $M_i=14.7nH$, $L_i=2.4\mu H$, and $k^2 \approx 0.85$. The SQUID occupies an area of <0.05 mm^2, not counting bonding pads. Only marginally less impressive are designs with $a=0.35\mu m$ and $a=0.5\mu m$ corresponding to excimer laser and i-line projection lithography capability.

As mentioned previously the small overall size of the washer is advantageous from the point of view of operating in a non-zero magnetic field B. Near the edges of the washer we can expect magnetic fields[20] of order $B(d+w)/t$, where t is the washer thickness. Our compact design minimizes (d+w). In addition by fabricating the washer last in the process sequence, one has the option of increasing t, thus further decreasing the magnetic field at the washer edges and minimizing deleterious flux penetration effects.

Finally some comments concerning the shape of the washer itself are in order. We find no compelling reason for any particular geometry. Ease of layout favors a square washer while aesthetics seems to favor a round washer. From a lithographic standpoint a circular spiral looks like a large set of equal lines and spaces which should have a higher yield at minimum dimensions than equal lines and spaces with many 90° turns that exist with a square spiral. A reasonable compromise is an octagonal design which retains most of the lithographic and aesthetic advantages of the circular design but requires far fewer points to specify.

Summary

We have reviewed the considerations for scaling planar dc SQUID designs into the deep sub-μm regime. There is easily room for an order of magnitude or more improvement in energy sensitivity and the basic coupling concepts now well verified at the 2-5μm level continue to apply down to dimensions of 0.1μm or less. In general at the 0.1-0.25 μm level we find SQUIDs that are smaller, quieter, friendlier, and better matched to input and output than their >1μm counterparts.

This work was partially conducted under the auspices of the Consortium for Superconducting Electronics.

References

1. J.M. Jaycox and M.B. Ketchen, IEEE Trans. Magn. MAG-17, 400 (1981); M.B. Ketchen and J.M. Jaycox, Appl. Phys Lett. 40, 736 (1982).
2. C.D. Tesche and J.Clarke, J. Low Temp. Phys. 29, 301 (1977).
3. M. Gurvitch, M.A. Washington and H.A. Huggins, Appl. Phys. Lett. 42, 472 (1983).
4. H. Kroger, L.N. Smith and D.W. Jillie, Appl. Phys. Lett. 39, 280 (1981).
5. M.B. Ketchen, M.Bhushan, S.B. Kaplan, and W.J. Gallagher, "Low Noise dc SQUIDs Fabricated in $Nb-Al_2O_3-Nb$ Trilayer Technology", these proceedings.
6. M.W. Cromar and P. Carelli, Appl. Phys. Lett. 38, 723 (1981); P. Carelli and V. Foglietti, J. Appl. Phys. 53, 7592 (1982).
7. V. Radhakrishnan and V.L. Newhouse, J. Appl. Phys. 42, 129 (1971).
8. J.H. Claassen, J. Appl. Phys. 46, 2268 (1975).
9. M.B. Ketchen, IEEE Trans. Magn. MAG-17, 387 (1981).
10. D.J. Van Harlingen, R.H. Koch, and J. Clarke, Appl. Phys. Lett. 41, 197 (1982).
11. W.C. Stewart, Appl. Phys. Lett 12, 277 (1968).
12. D.E. McCumber, J. Appl. Phys. 39, 3113 (1968).
13. V. Foglietti, W.J. Gallagher, M.B. Ketchen, A.W. Kleinsasser, R.H. Koch, and R.L. Sandstrom, Appl. Phys. Lett. 55, 1451 (1989).
14. J.M. Martinis and R.H. Ono, Appl. Phys. Lett., 57, 629 (1990).
15. Shin'ichi Morohashi, Shinya Hasuo and Toyoshi Yamaoka, Appl. Phys. Lett. 48, 254 (1986).
16. S. Nagasawa, H. Tsuge and Y. Wada, IEEE El. Dev. Lett. 9, 414 (1988).
17. F.C. Wellstood, C. Urbina, and J. Clarke, IEEE Trans. Magn. MAG-25, 1001 (1989).
18. W.H. Chang, J. Appl. Phys. 50, 8129 (1979).
19. M.B. Ketchen, W.J. Gallagher, A.W. Kleinsasser, S. Murphy and J.R. Clem in SQUID '85, edited by H.D. Hahlbohm and H. Lubbig (Walter de Gruyter, Berlin, New York, 1985), 865.
20. R.P. Huebener, R.T. Kampwirth, and J.R. Clem, J. Low Temp. Phys. 6, 275 (1972).